



## THE EFFECT OF LEADING EDGE PROTUBERANCES ON THE PERFORMANCE OF SMALL ASPECT RATIO FOILS

J.-H. CHEN<sup>1,c</sup>, S.-S. LI<sup>1</sup>, V.T. NGUYEN<sup>1,2</sup>

<sup>1</sup> Department of Systems & Naval Mechatronic Engineering, National Cheng Kung University, Tainan, 70101, Taiwan

<sup>2</sup> Faculty of Transportation Mechanical Engineering, Da Nang University of Technology, Da Nang, Vietnam

<sup>c</sup> Corresponding author: Tel.: +886-62747018#210; Fax: +886-62747019; Email: chenjh@mail.ncku.edu.tw

### KEYWORDS:

**Main subjects:** leading edge, protuberances

**Visualization method(s):** oil film

**Other keywords:** turbulence, aspect ratio

**ABSTRACT:** Inspired by humpback whale's flippers [1, 2], this study investigated the effect of aspect ratio and shape of protuberances on the performance of airfoil with protuberances on leading edge. NACA0012 foil is used for modifying the leading edge with three different forms and three aspect ratios (1, 2, 3). The experiment of the airfoils was carried out in a low-speed wind tunnel, including airfoil performance measurements and visualization of airfoil surface flow field by oil film. The results of performance experiments show that when the aspect ratio equal to 1, the stall-delay phenomenon is very clear. It means that it is more useful than the high AR foil at high attack angle. The airfoil performance with protuberances on leading edge has no significant increase in lift, but the drag was reduced. The most significant effect for performance took place for the foil with longest amplitude of the protuberances. The flow visualization results show that the airfoil's flow field becomes very turbulent on the wing surface after stall angle. But the protuberance foil's flow field distribution was regular. From the difference between these two results, one could conclude the reason why the leading edge protuberance delayed stall and reduce the drag. The results of CFD simulation by Star-CCM+ was also accordant to experiments. The results will provide some base for the application of small aspect ratio wing with leading edge protuberances to the situations with a wide range of attacking angle.

### INTRODUCTION

The idea of changing the leading edge of air-/hydrofoils to resemble the leading edge of the humpback whale flipper was firstly inspired by the prior work of marine biologists who studied the morphology of the humpback whales pectoral flippers. Despite its enormous size (adults ranging from 12-16m), the humpback whale is quite maneuverable compared to other species of whale. It has been determined by biologists such as Fish [1, 2] through qualitative visualization of the humpback whale in nature that it can be said that the humpback whale has superior maneuverability in term of turning radii and its movement in water relative to aquatic animals of comparable size. This maneuverability has been attributed to the use of their pectoral flippers.

Fish and Battle report that humpback whale flippers have large aspect ratios ( $s/c \approx 6$ ,  $s$ =span,  $c$ =chord length) as well as the large scale protuberances located along the leading edge [1]. There is speculation that the protuberances act as a form of passive flow control. For most of the humpback whales their flipper has a quasi-symmetric profile. The thickness ratio of the flipper ranges from 0.2 to 0.28 of the chord length, with an average value of 0.23  $c$ , where the thickness ratio decreases from the mid-span to the tip. The maximum thickness ratio locates from 0.20  $c$  to 0.40  $c$ . The cross-section of the flipper has a profile similar to the NACA 63<sub>4</sub>-021. Following the previous research, more studies were carried out to find its effects and mechanisms. The protuberances found along the leading edge of the humpback flipper vary in amplitude and wavelength with span. The amplitude of the protuberances ranges from 2.5 to 12% of the chord length and the wavelength varies from 10 to 50% of the chord. It has been hypothesized protuberances act as a form of passive flow control [1] and/or a form of drag deduction [3].



An examination of the effects of leading edge protuberances on the load characteristics of a low aspect ratio wing using numerical methods was performed by Watt and Fish [4]. This study formed that at  $\alpha=10^\circ$ , 4.8% increase in lift was generated by a wing with protuberances over a baseline wing without protuberances. A study on the characteristics of a humpback whale flipper model in a wind tunnel done by Miklosovic et al.[2] reported a 6% increase in the maximum lift and a 40% increase in the stall angle over the baseline wing. Their results also show that over the range of  $10^\circ \leq \alpha \leq 18^\circ$  there is an overall decrease in drag when protuberances are present. This implies that protuberances, in essence, create a more efficient wing over certain range of angle of attack. Specially, the post-stall angles of attack of the baseline model, show significant increases in the lift to drag ratio. Another study by Stein and Murray [5] reported that a two-dimensional airfoil with protuberances whose amplitude and wavelength equal to the average amplitude and wavelength of the humpback whale flipper, results in a significant loss in lift and a large increase in drag. Their measurement was done at the angle of attack ranging from  $8^\circ$  to  $12^\circ$ . The difference between the Stein and Murray's experiment and others is that Stein and Murray tested two-dimensional airfoils whereas the others tested finite wings. It is possible that the present of protuberances on the finite wings may have affected the spanwise flow over the wings. The effects of adding leading edge sweep on humpback whale flipper was reported an enhanced aerodynamic performance with increasing sweep angle as expected.

For the wings considered in this study, the introduction of protuberances on the leading edge altered the entire flow field over the wing, and was expected to have more effects than that of the previously observed drag reduction. Miklosovic et al. [2] did the tests with a full-span model pair and a semi-span model pair in two different wind tunnels. Although the aerodynamic mechanisms of the scalloped leading edges are similar, the effects were vastly different between the infinite wing and finite wings. The substantial loss in lift and increase in drag that accompanied the full-span results, but not the semi-span results, means that the scallops had largely a 3-D benefit that is a function of the platform shape and the Reynolds number. At pre-stall angle of attack, the trends were the same (decrease in lift and moment, increase in drag) but the 3-D effects were much smaller in magnitude. The post-stall behavior showed the opposite trends as a result of the scallops: increasing lift and moment, decrease drag. Johariet et al. [6] examined the flow field on hydrofoils with leading edge protuberances similar to those in humpback whale flippers. Flow visualization experiments were conducted in a water tunnel. Both dye injection and surface tufts were for the assessment of the flow patterns on symmetry with respect to the protuberances at low angles of attack and the formation of streamwise vortices. The flow patterns and the stall cells were not stationary at Reynolds numbers of  $\sim 10^5$  as depicted by the tufts, and the formation of stall cells and separated regions was delayed to greater angle of attack when compared with the dye visualization experiments at Reynolds numbers of  $\sim 10^4$ . Both flow visualization techniques revealed that the flow over the peaks of protuberances remained attached at angles of attack greater than  $20^\circ$  while flow separation occurred first behind the troughs on the modified hydrofoil.

Van Nierop et al. [7] explained how bumps on whale flippers delay stall. Their wind tunnel experiments have shown that bumps on the leading edge of model humpback whale flippers cause them to "stall" more gradually and at a higher angle of attack. Here they develop an aerodynamic model which explains the observed increase in stall angle. The model predicts that as the amplitude of the bumps is increased; the lift curve flattens out, leading to potentially desirable control properties. They find that stall delay is insensitive to the wavelength of the bumps, in accordance with experimental observations. Pedro [8] then simulated numerically the wind tunnel experiments for two different wings inspired in the humpback whale flipper. One of the flippers displays a scalloped leading edge whereas the other one has a smooth leading edge. The experimental study revealed a significant increase in the aerodynamic performance for the scalloped flipper close to the separation. The detailed numerical solution allows for the complete characterization of the flow



for both flippers. Levshin et al. [9] used NACA 63<sub>4</sub>-021 foil section to investigate this problem experimentally, and found that the protuberances did not delay the stall. However, the lift was higher than smooth leading edge case in stall region and the drag is not higher when attack angle larger than 5 degree. The amplitude of protuberances affects the flow more than wave length. The flow separation between protuberances is the main reason for the lift increasing in stall region. Similar founding is also obtained by simulation by Pedro and Kobayashi [10].

The application to hydrodynamic purpose is less seen. Weber et al. [11] used NACA0016 section to study rudder (low aspect ratio) performance and cavitations problem comparing normal smooth leading edge and leading edge with protuberances. Their experiments show that protuberances increase the cavitations, and also change the location of cavitations. In addition to tip cavitations, unlike normal rudder, protuberances also make cavitations to concentrate at the valleys of leading edge. They also found that lift is decreased and drag is increased between 15 and 22 degrees of attack angle, while the lift is larger at 22 degree and above. They also found that the differences between normal wing section and wing with leading edge protuberance are not significant at higher Reynolds number. Table 1 is the summary of past research conditions.

Table 1 Past research conditions

Year	Author	Research methods	Wing section	Aspect Ratio	Protuberance wave Length ( $\lambda/C$ )	Protuberance Amplitude ( $A/C$ )
1995	Fish et al.	Experiment	NACA 63-021	6.1	-	-
2001	Watts et al.	Simulation	NACA 63 <sub>4</sub> -021	2.04	-	-
2004	Miklosovic et al.	Experiment	NACA 0020	8.7	0.04	0.47
2007	Miklosovic et al.	Experiment & Simulation	NACA 0020	3.29 ; 4.06	0.04	0.47
2007	Levshin et al.	Experiment	NACA 63 <sub>4</sub> -021	2	0.025;0.05;0.12	0.25;0.5
2008	Ernst et al.	Experiment	NACA 63 <sub>4</sub> -021	2.5	0.025;0.05;0.12	0.25;0.5
2008	Pedro et al.	Simulation	UAV's wing	4.4	-	-
2010	Weber et al.	Experiment	NACA 0016	1.6	0.0625;0.14	0.26;0.44

Considering the possible applications to marine hydrodynamics purpose, namely control fins and rudders, the purpose of this study concentrated on low aspect ratio case of wings having leading edges with protuberances, because the control fins and rudders of any marine vehicles can't be too long due to space limit and safety reasons. Past researches, as reviewed in the above, provide much more information about large aspect ratio and 2D wing sections than low aspect ratio cases. Hence, the objective of this research is to study the effects of various shapes of protuberances on low aspect ratio wings experimentally and numerically.

## EXPERIMENTAL METHODS

First, to study various shapes of protuberances, we have to systematically define the geometry of protuberances. The wing section is separated into two parts at the maximum thickness location. For the section used in this study, NACA 0012, that is  $x=0.3c$  where  $c$  is the chord length. The upper surface and lower surface at this location are named P1 and P2, respectively. The surfaces are then defined by NACA 4 digit definition for  $x/c > 0.3$ , and defined by an elliptical equation for  $x/c < 0.3$ . The outline shape of protuberances is defined by a sinusoidal function. The amplitude,  $A$ , and wave length,  $\lambda$ , are also normalized by chord length  $c$ .

The protuberance is generated by modifying chord length periodically along span wise direction. The difference of chord length between modified and original ones is defined as  $\Delta c$ . Then, the upper and lower surfaces can be defined as:



$$y_u = b \sqrt{1 - \left( \frac{x - 0.3c}{a} \right)^2}, \Delta c \leq (x/c) \leq 0.3 \quad (1)$$

$$y_l = -b \sqrt{1 - \left( \frac{x - 0.3c}{a} \right)^2}, \Delta c \leq (x/c) \leq 0.3 \quad (2)$$

where  $a = 0.3 - \Delta c$  and  $b$  is the half maximum thickness, also representing the length of long axis and short axis of an ellipse, respectively. The change of chord length  $\Delta c$  is defined by the following wave equation:

$$\Delta c = \frac{A}{2} \left( 1 + \sin\left(\frac{2\pi z}{\lambda}\right) \right) \quad (3)$$

where  $A$  is the amplitude and  $\lambda$  is the wave length. Hence, the geometry of modified wing can be defined. The sectional view and top view is seen in Figure 1. In this study, three amplitudes were used  $A/c = 0.05, 0.1,$  and  $0.15$ . Only one wave length is used:  $\lambda = 0.25c$ . The wing sections are named NACA0012S, NACA0012M, and NACA0012L for  $A/c = 0.05, 0.1,$  and  $0.15$ , respectively. The models are seen in Figure 2. A typical comparison between original NACA 0012 section and modified ones is shown in Figure 3. Notice that there is a small difference near leading edge. The aspect ratio studied includes 1, 2, and 3.

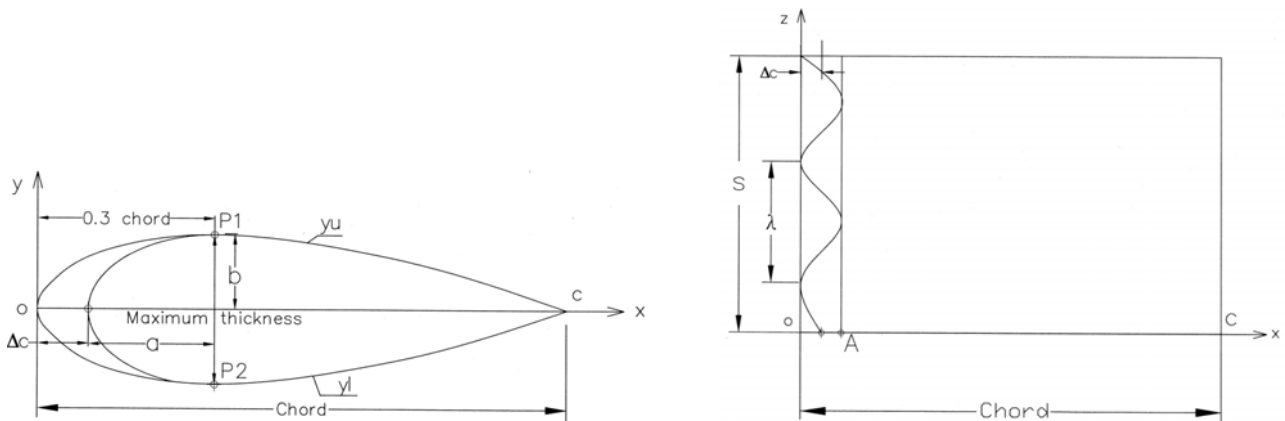


Figure 1 The sectional view (left) and top view (right) of wing geometry.

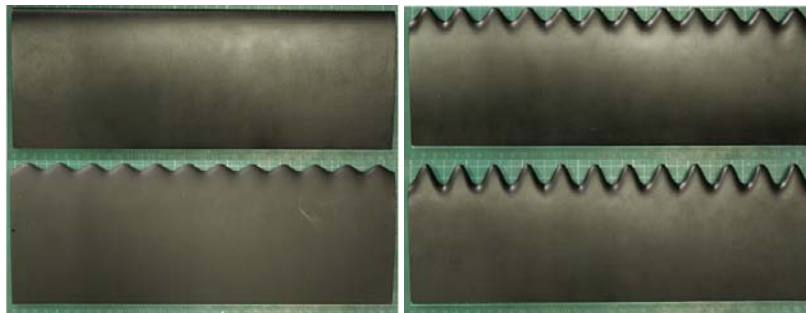


Figure 2 Experimental model with section of NACA0012 of aspect ratio 3 (top left), NACA0012S (bottom left), NACA0012M (top right), and NACA0012L (bottom right)

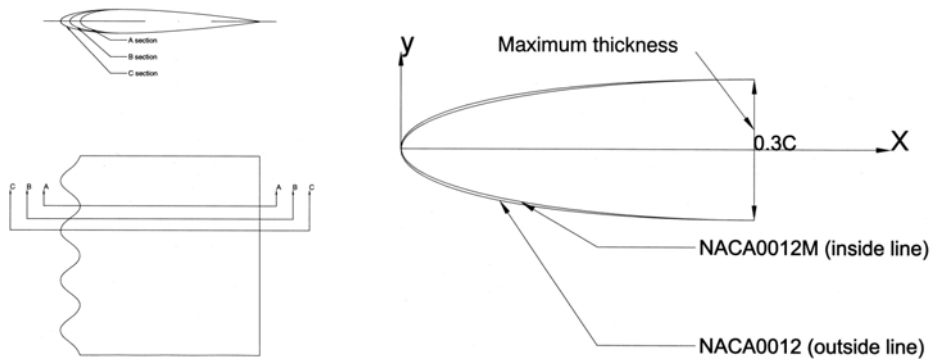


Figure 3 The difference between original NACA section and modified section.

The experiment consists of two parts, the performance measurement and flow visualization. Both parts use the same model and apparatus and were carried out in the low speed wind tunnel in Dept. of Aerospace Engineering, National Cheng Kung University. Its test section of the wind tunnel is 4.40m long, 1.22m wide, and 0.914m high. The contraction ratio of 9:1 and several screens provide low turbulent inflow (<1%) of 5~30m/s. The mean velocity is measured by Pitot tube, pressure transducer and micro-manometer system. The performance measurement includes lift and drag. Both forces were measured by a six-component force gauge made by Jeou Rong Industrial Co. with maximum load of 10N of force. The analog signal was converted by an 8-channel A/D converter with  $10^4$ Hz maximum sampling rate (Io-Tech) before captured and stored by computer software. The attack angle was controlled by a home-made Parallax Servo controller with precision of 0.2 degree.

The flow visualization part was carried out by oil film using a mixed solution consisting of titanium dioxide ( $\text{TiO}_2$ ), kerosene, and oleic acid with a mass ratio of 3:6:2 which is the best testing result. This mix solution let titanium dioxide be resolved in kerosene and oleic acid, and then stick on the wing surface after oleic acid evaporates. A digital camera (Sony, HDR-SR11) was used to capture the image of surface flow pattern formed by titanium dioxide residuals. Flow visualization was chosen only at some attack angles at which the wing is before, during, and after stall. Due to time limit, only NACA 0012 and NACA 0012M sections were selected to be visualized for all aspect ratios, in order to compare their difference. All the test conditions and measurement uncertainties for each condition are summarized in Table 2. Attack angles are adjusted for aspect ratio and wing performance. The Reynolds number based on chord length is  $1.23 \times 10^5$ . All measurement uncertainties are below 5%.

Table 2 Experiment conditions

Aspecr Ratio	Section	Attack Angle	Flow Visualizatin	Inflow (m/s)	$Re_c$	Measurement Uncertainty			
						$C_L$ (%)	$C_D$ (%)	L/D (%)	$Re_c$ (%)
AR=1	NACA 0012	0°~40°	30°, 34°, 40°	15	$1.233 \times 10^5$	2.9	3.2	3.2	2.0
	NACA 0012S	0°~40°	30°, 35°, 40°			2.6	3.4	3.3	2.0
	NACA 0012M	0°~40°	30°, 32°, 40°			2.5	3.2	2.9	2.0
	NACA 0012L	0°~40°	-			2.8	3.1	3.1	2.0
AR=2	NACA 0012	0°~20°	14°, 16°, 18°	15	$1.233 \times 10^5$	3.1	4.1	4.3	2.0
	NACA 0012S	0°~30°	-			3.0	3.9	4.1	2.0
	NACA 0012M	0°~30°	14°, 16°, 18°			3.3	3.9	4.3	2.0
	NACA 0012L	0°~35°	-			3.1	3.9	4.2	2.0
AR=3	NACA 0012	0°~20°	13°, 15°, 17°	15	$1.233 \times 10^5$	3.5	4.3	4.8	2.0
	NACA 0012S	0°~25°	-			2.8	3.8	3.8	2.0
	NACA 0012M	0°~25°	13°, 15°, 17°			3.3	4.9	5.1	2.0
	NACA 0012L	0°~30°	-			3.6	4.1	4.7	2.0



## RESULTS AND DISCUSSION

### Performance

Figure 4~9 show the lift and drag coefficients and lift-to-drag ratio of various wing sections for three aspect ratios at different attack angles, respectively. The symbol sizes are roughly the same as their measurement uncertainty level of attack angle, such that the error bar in the figure is omitted in abscissa, while the error bar for lift and drag coefficients are shown in the figures. Form these figures we can compare the effects of the size of protuberances.

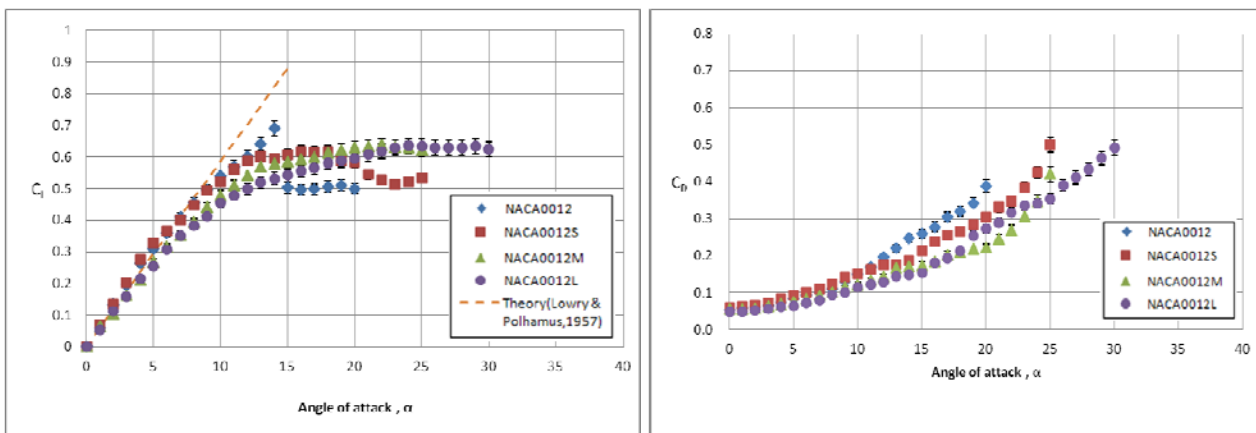


Figure 4 Lift and drag coefficients at various attack angles (AR=3)

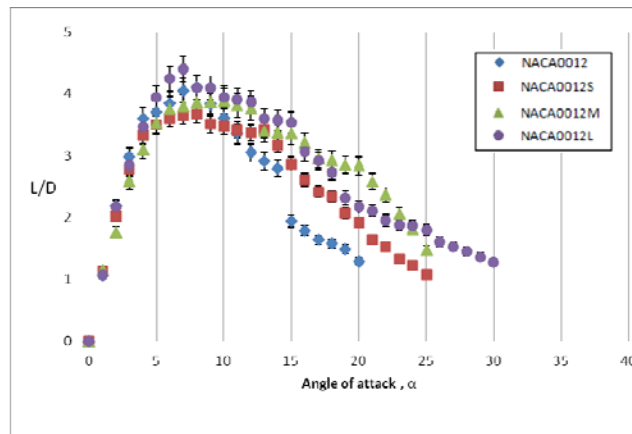


Figure 5 Lift-to-drag ratio at various attack angles (AR=3)

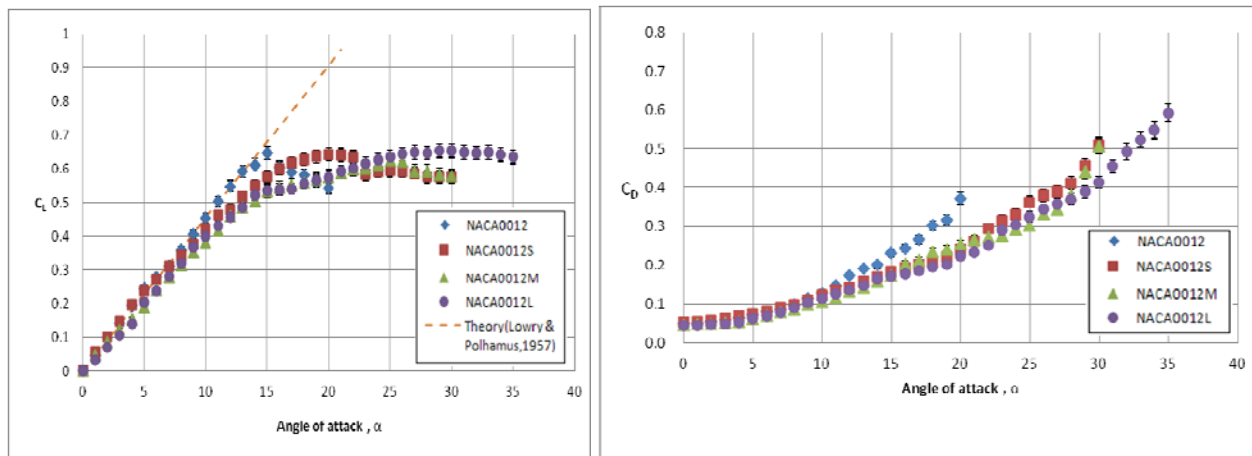


Figure 6 Lift and drag coefficients at various attack angles (AR=2)

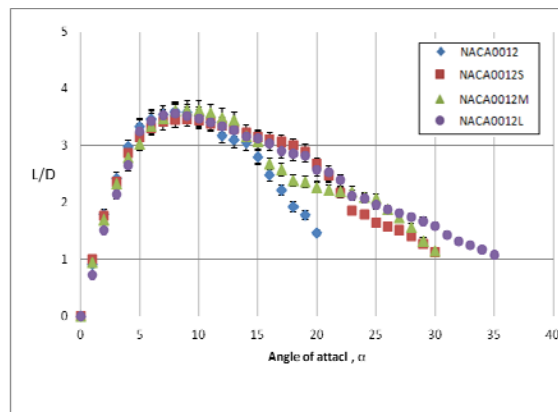


Figure 7 Lift-to-drag ratio at various attack angles (AR=2)

For aspect ratio 3, original NACA0012 wing stall at about 14 to 15 degree, while the stall angle for NACA0012S is delayed to 19~20 degree. NACA0012M still has a stall phenomenon at 22 degree, but not significant. NACA0012L has no observable stall. Its lift coefficient increases with attack angle till 25 degree and then stays a constant till 30 degree. The larger the modification, the more delay of stall angle. But the lift coefficients of modified wings are all smaller than original one before stall angle. The more modified (large protuberance amplitude), the less lift coefficients. The drag coefficients are similar at low attack angles. But modified wings have slightly smaller drag than original ones at attack angle larger than 10 degree. The drag decreases opposite to the modification degree, expect that NACA0012L has larger drag than NACA 0012M after 23degree. Similar trends can be observed in the case of aspect ratio 2 and 1. The difference among various aspect ratios is that the stall angle increases when aspect ratio decreases. As to the efficiency, the lift-to-drag ratio shows that after original stall angle, the efficiency of modified wings are all better than NACA0012. But the difference is not large for aspect ratio of 1. Another way to analyze the same results is to observe the effect of aspect ratio on various wings. This might be important when designing a control fin. It is obvious that the smaller aspect ratio has higher stall angle, but smaller lift coefficient at the same attack angle.

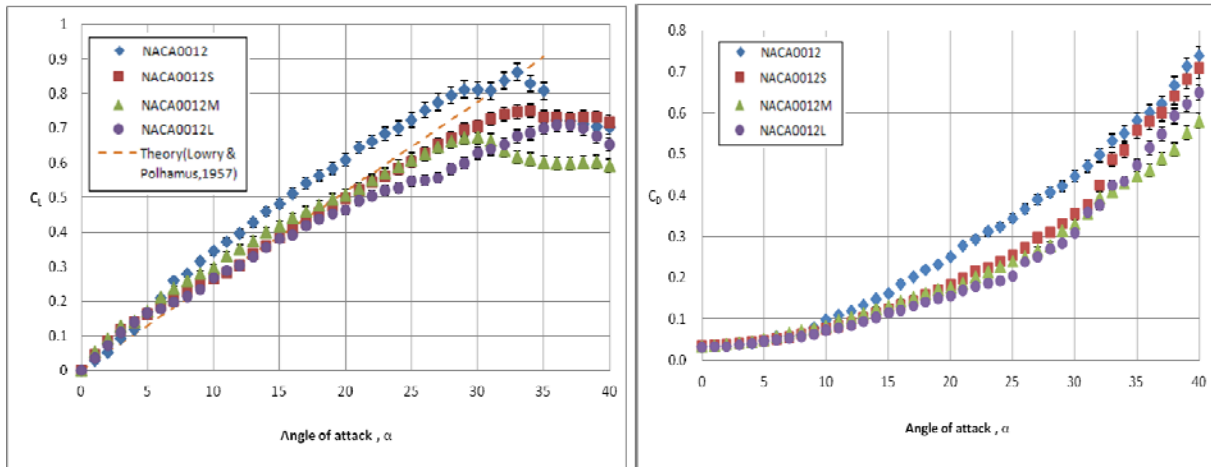


Figure 8 Lift and drag coefficients at various attack angles (AR=1)

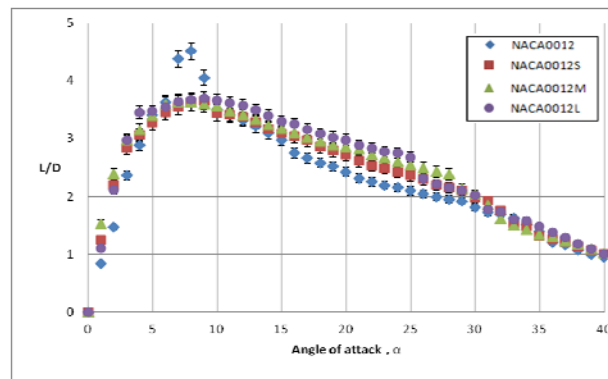


Figure 9 Lift-to-drag ratio at various attack angles (AR=1)

## Flow Visualization

Flow visualization results can be seen in figure 10~16 for comparison between NACA 0012 and modified wings of aspect ratio 3, 2, and 1, respectively. The location of significant flow structure, such as Separation, reattachment, separation bubble, and tip vortex, are all marked. By comparing the difference between NACA 0012 and modified wings, the flow structure can help to explain the performance differences. For aspect ratio of 3, the difference came from the location of separation. While NACA 0012 separate uniformly at the same location in chordwise direction, the protuberances make separation point varies periodically such that there is still a small area near leading edge without separation after stall angle that preserved some lift.

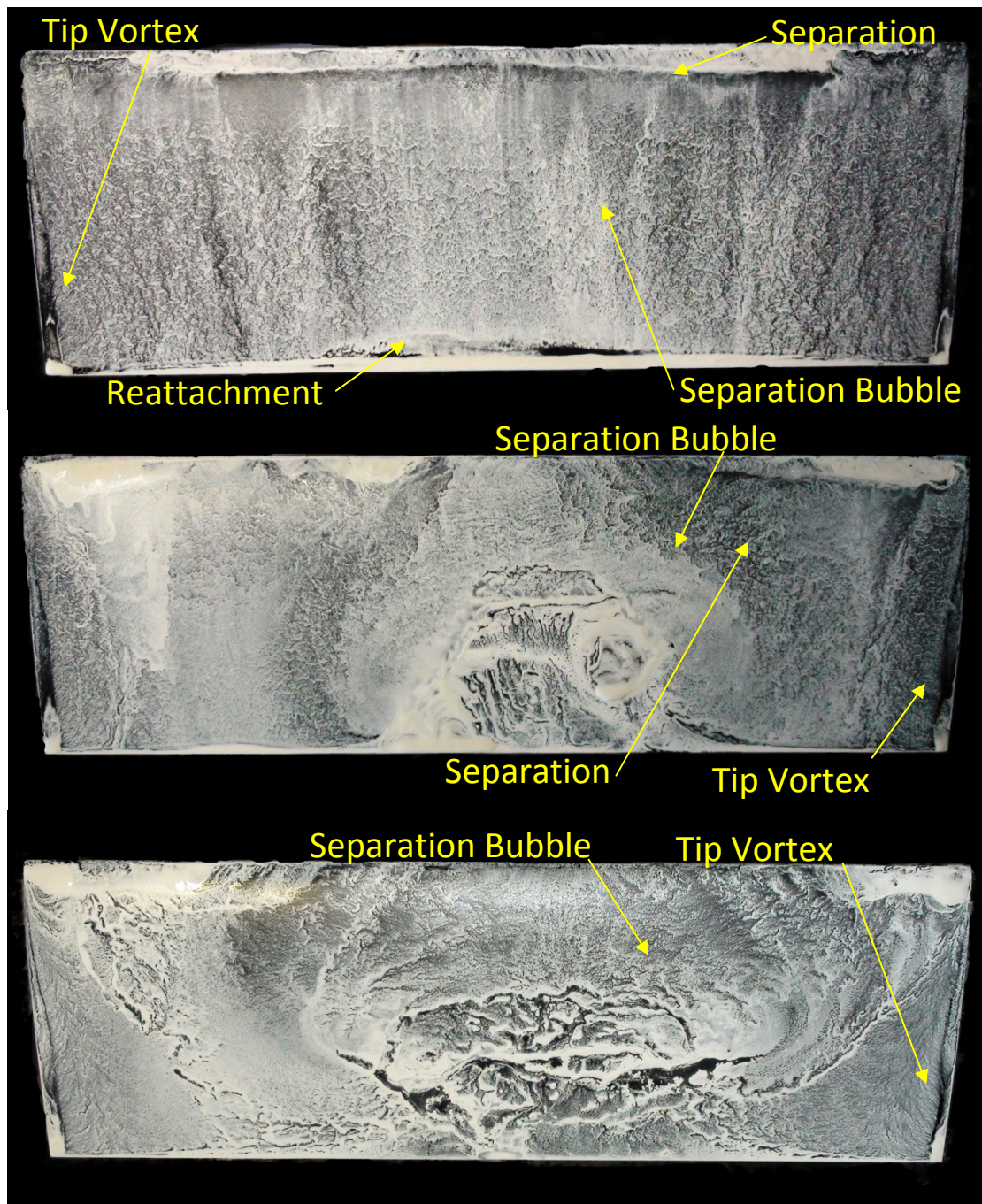


Figure 10 Flow visualization of NACA0012 (AR=3)  $\alpha=13^\circ$ ,  $15^\circ$ , and  $17^\circ$  (top to bottom)

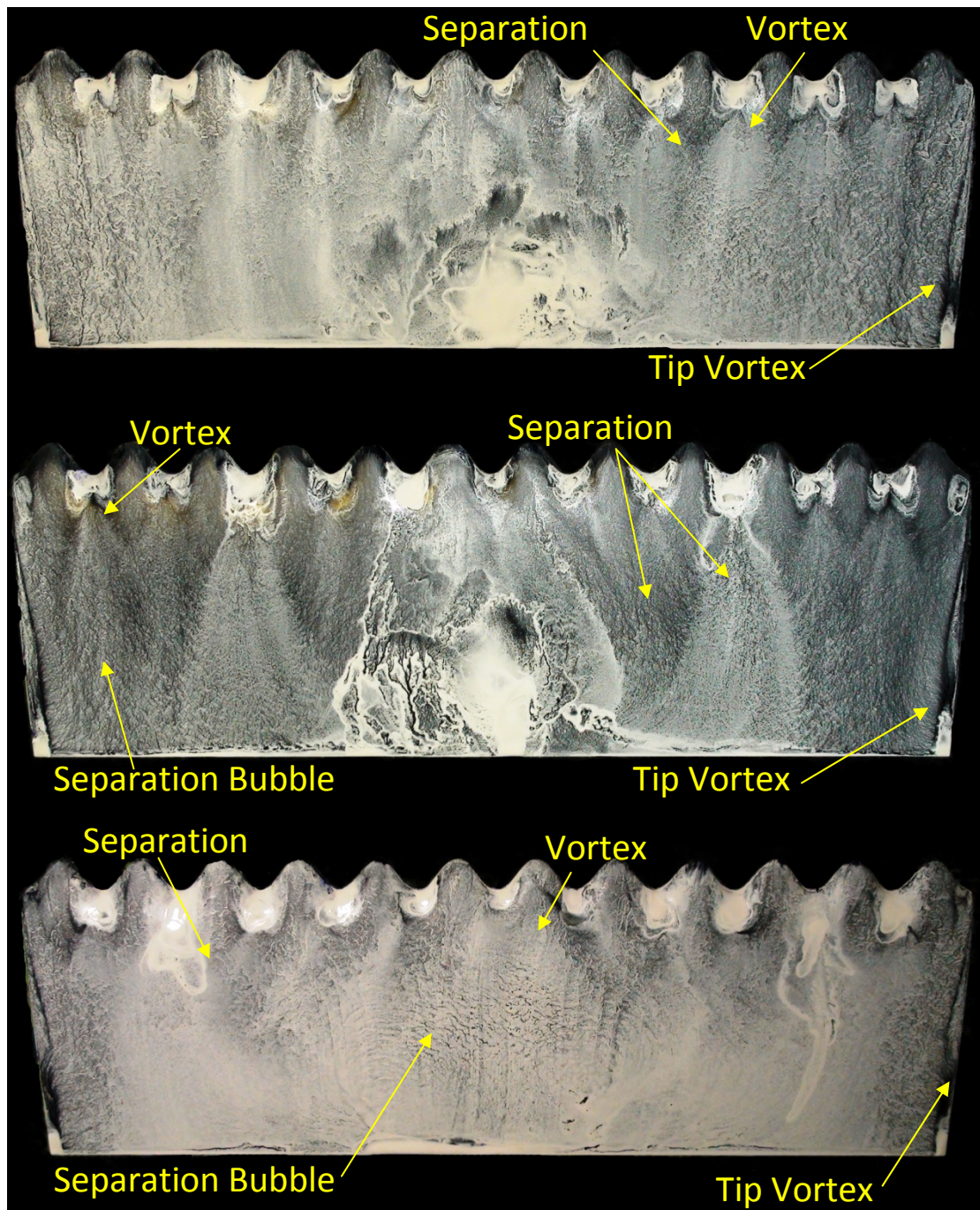


Figure 11 Flow visualization of NACA0012M (AR=3)  $\alpha=13^\circ, 15^\circ, 17^\circ$

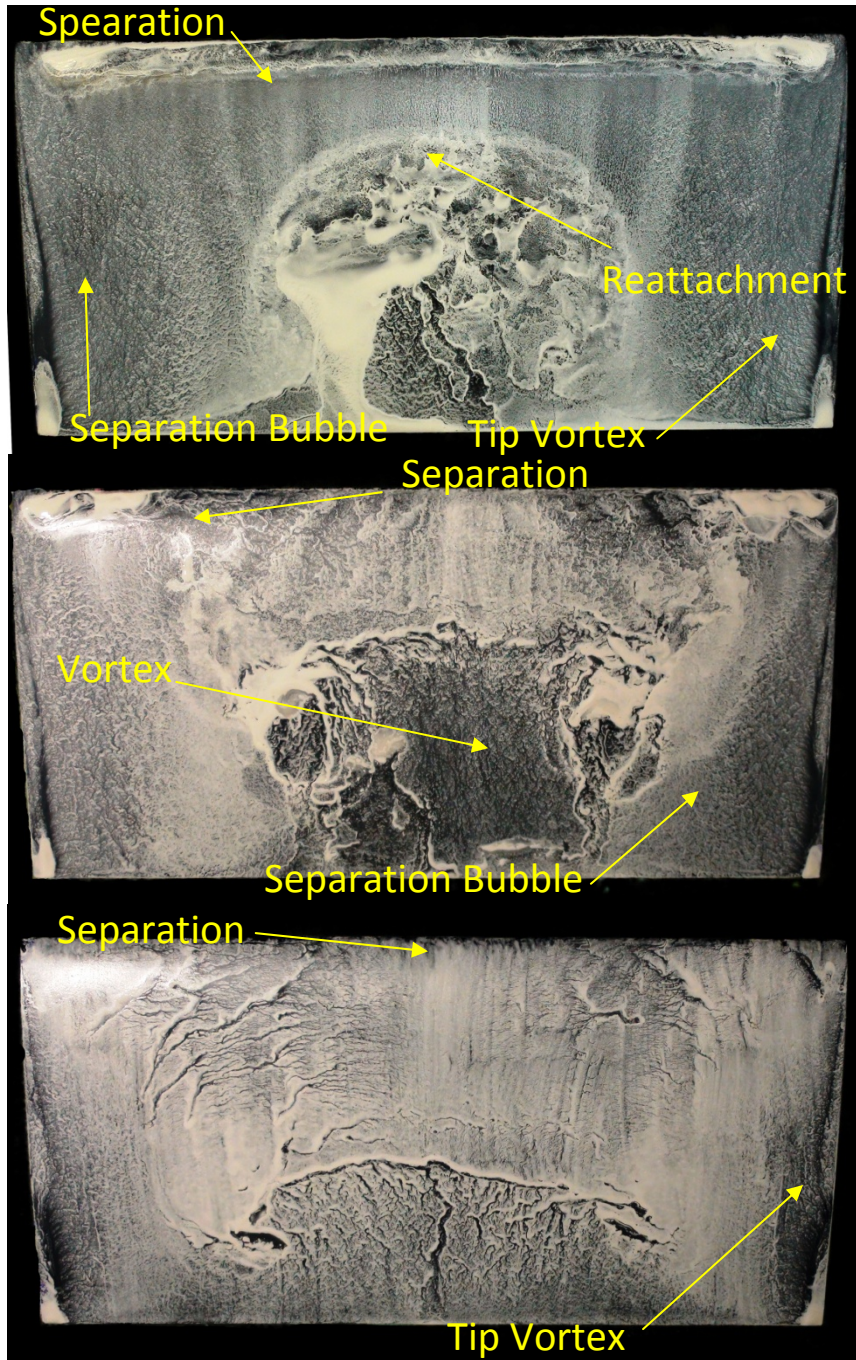


Figure 12 Flow visualization of NACA0012 (AR=2)  $\alpha=14^\circ, 16^\circ, 18^\circ$

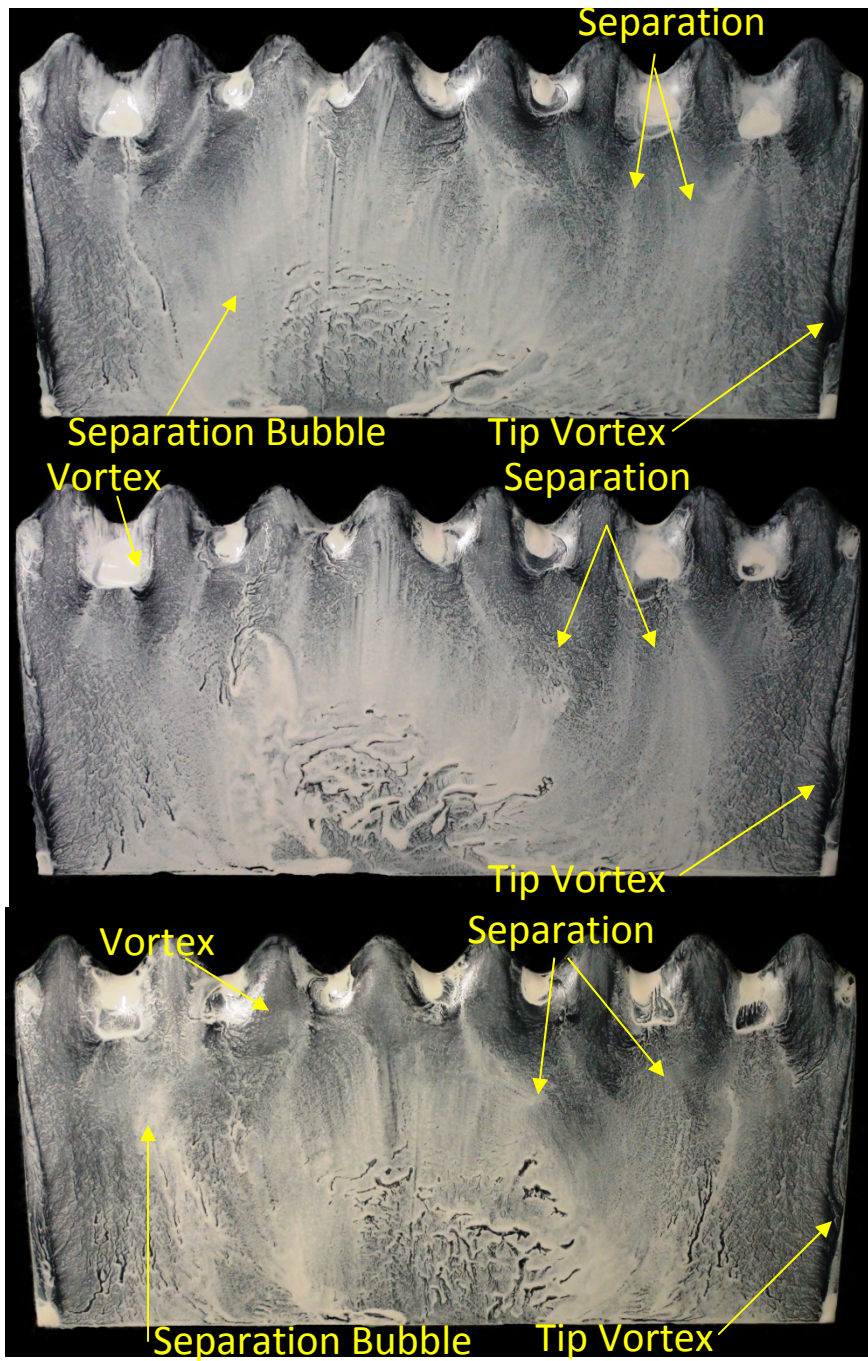


Figure 13 Flow visualization of NACA0012M (AR=2)  $\alpha=14^\circ, 16^\circ, 18^\circ$

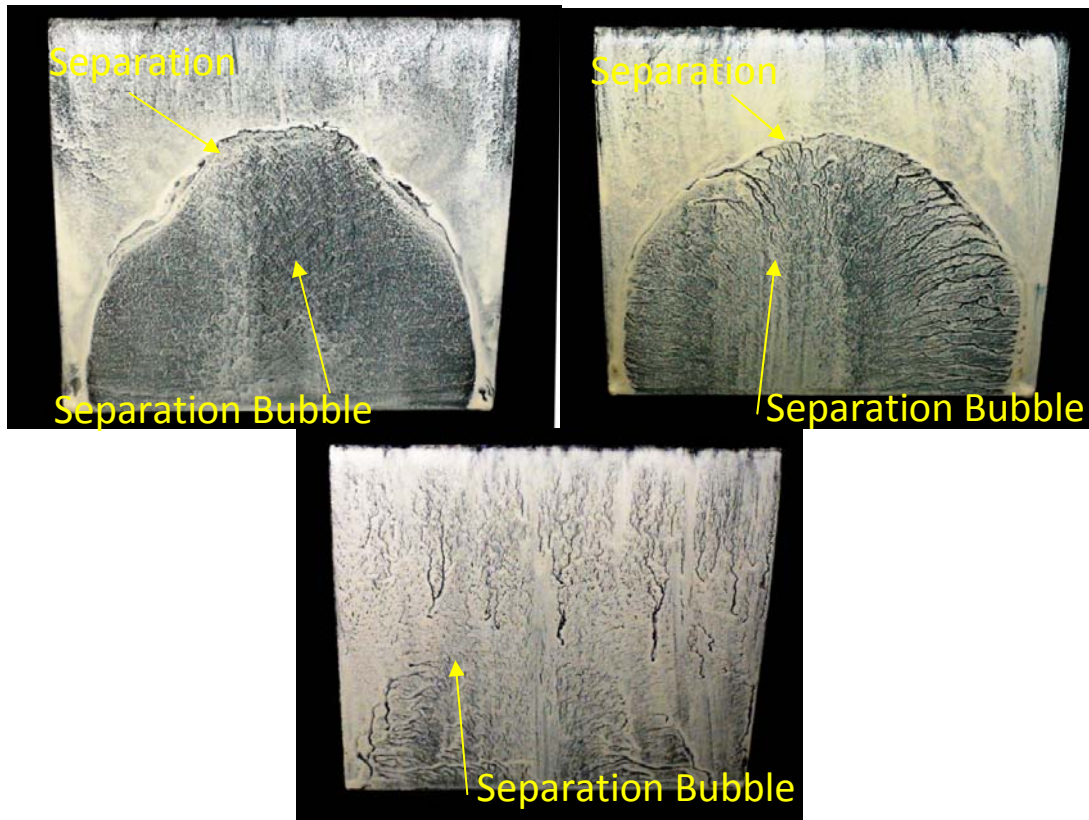


Figure 14 Flow visualization of NACA0012 (AR=1)  $\alpha=30^\circ, 34^\circ, 40^\circ$

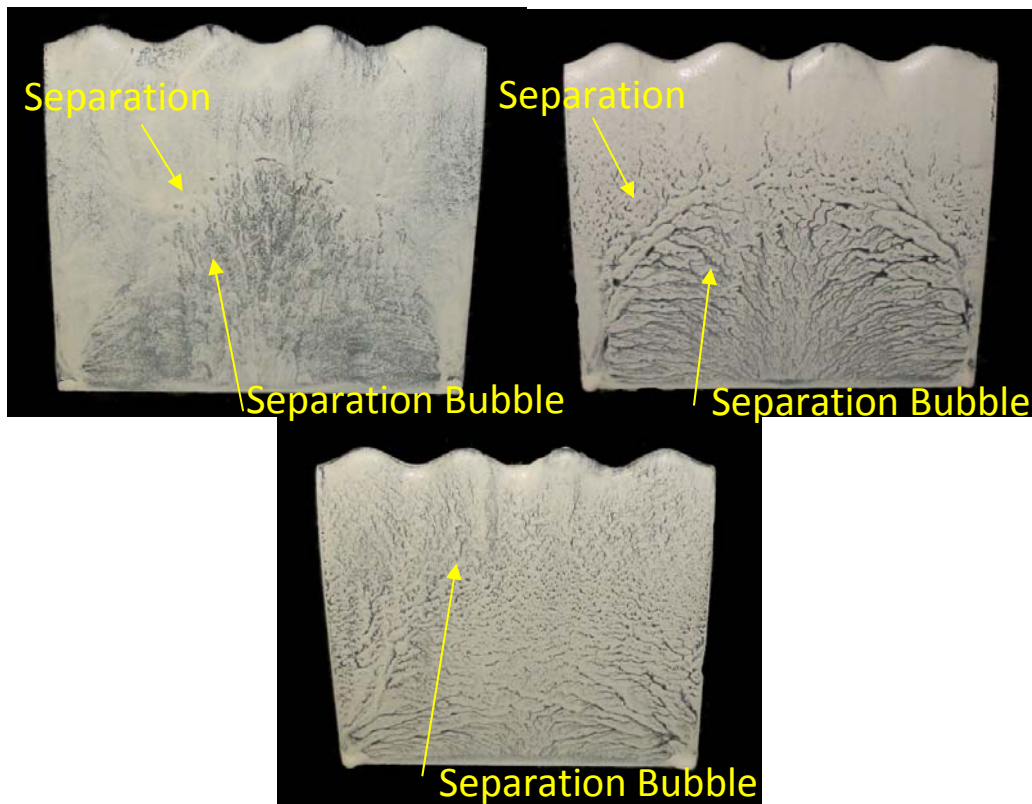


Figure 15 Flow visualization of NACA0012S (AR=1)  $\alpha=30^\circ, 35^\circ, 40^\circ$

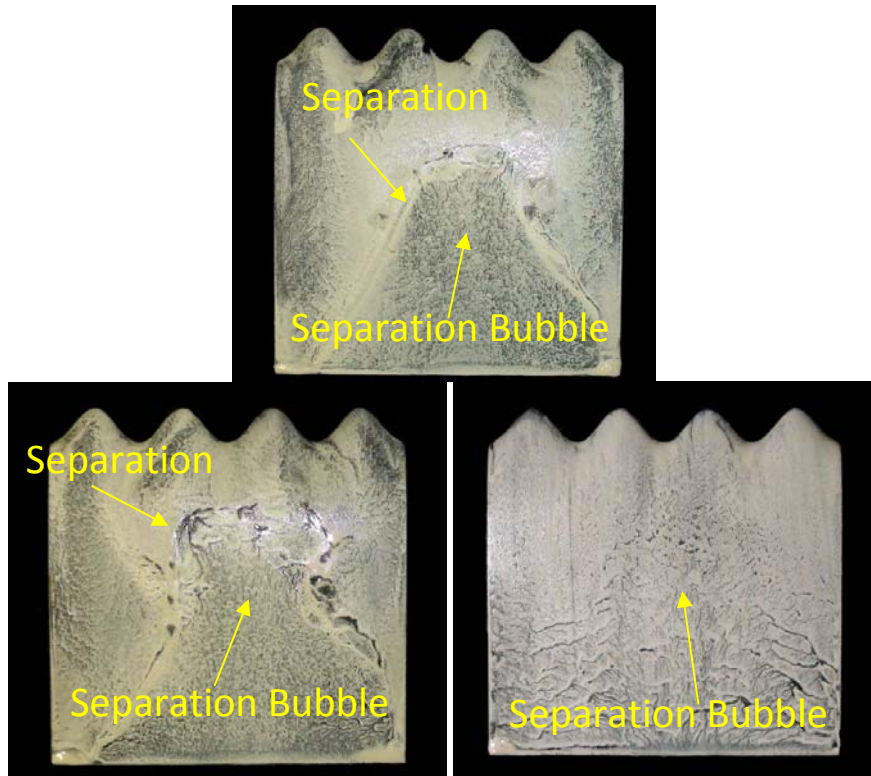


Figure 16 Flow visualization of NACA0012M (AR=1)  $\alpha=30^\circ, 32^\circ, 40^\circ$

## Discussion

For small aspect ratio of 1, we can see this trend more clearly due to the obvious separation area on both wings. It is very clear that NACA 0012 has a larger separation area, while the modified wing's separation area seems squeezed in more center region near the leading edge. Table 3 summarizes the maximum lift coefficients, maximum L/D and corresponding attack angles for various wings and aspect ratios. It is obvious that the stall angle become larger, which is usually called "the delay of stall". However, its maximum lift coefficients are smaller than original wing. Comparing the results of same aspect ratio, we can also find that large protuberance (NACA0012L) has largest drag reducing effect. This is different from Levshin et al. [9] who used wing section of NACA 63<sub>4</sub>-021 with aspect ratio of 2, but the same for the L/D raises in stall region. Notice that current results are similar to Miklosovic et al. [2, 12] on the reduction of drag, stall delay, and increase of L/D.

Table 3  $C_{L,max}$ ,  $L/D_{max}$  and corresponding attack angle

Aspect Ratio	Wing	$C_{L,max}$	$\alpha_{C_{L,max}}$	$L/D_{max}$	$\alpha_{L/D_{max}}$
AR=1	NACA 0012	0.86	33°	4.52	8°
	NACA 0012S	0.75	34°	3.65	9°
	NACA 0012M	0.68	30°	3.63	7°
	NACA 0012L	0.71	37°	3.69	9°
AR=2	NACA 0012	0.65	15°	3.6	8°
	NACA 0012S	0.64	20°	3.47	9°
	NACA 0012M	0.63	25°	3.62	9°
	NACA 0012L	0.65	29°	3.56	8°
AR=3	NACA 0012	0.69	14	4.11	8°
	NACA 0012S	0.62	16	3.67	8°
	NACA 0012M	0.64	22	3.89	10°
	NACA 0012L	0.64	24	4.41	7°



It should be noted that in addition to what pictures shows, we also observed that separation, there is a recirculation from trailing edge to the valley near leading edge. Vortices also appear in the valleys. Flow then spared out from valleys, like the tuft pattern seen by Levshin et al. [9] The turbulence in the central region of upper surface appear to be more irregular on NACA 0012 than modified wings. This might need more quantitative studies to investigate the flow behavior and structure on and above the upper surface, in order to figure out its relationship with the drag reduction and stall delay phenomenon.

Moreover, we also conduct a preliminary simulation of these flows. The simulation used Star-CCM+ software using k-omega turbulence model. The vorticity and pressure pattern on upper surface are quite consistent with flow visualization result for NACA0012M with aspect ratio of 1. Figure 17 shows a typical result (left half only) at angle of attack 30°, when the separation just begin and stall occurs.

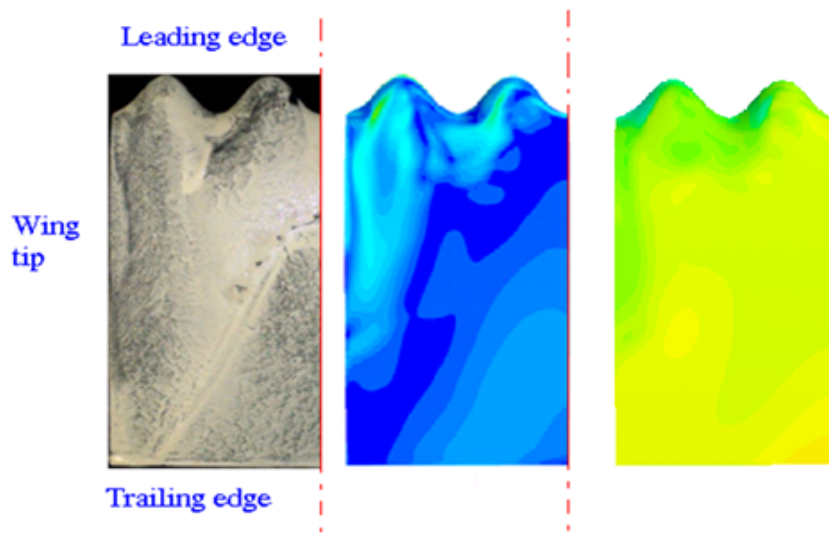


Fig. 17 Airfoil NACA 0012M with aspect ratio of 1 at angle of attack 30°. The separation bubble pattern shown by visualization (left) is consistent with vorticity (center) and pressure (right) distribution.

## CONCLUSION

In the present study, we mainly use experimental method to study the performance of wings with modified leading edges, which is inspired by humpback whale's flippers. The effect of aspect ratio and shape of protuberances on the performance of airfoil NACA0012 foil is investigated for three aspect ratios (1, 2, 3). The experiment of the airfoils was carried out in a low-speed wind tunnel, including airfoil performance measurements and visualization of airfoil surface flow field by oil film. The results show that when the aspect ratio equal to 1, the stall-delay phenomenon is very clear. It means that it is more useful than the high AR foil at high attack angle. The airfoil performance with protuberances on leading edge has no significant increase in lift, but the drag was reduced. The most significant effect for performance took place for the foil with largest amplitude of the protuberances. The flow visualization results also show that the airfoil's flow field becomes very turbulent on the wing surface after stall angle. But the protuberance foil's flow field distribution was relatively more regular. From the difference between these two results, one could conclude the reason why the leading edge protuberance delayed stall and reduce the drag. The results of CFD simulation by Star-CCM+ was also consistent to experiments. The results will provide some base for the application of small aspect ratio wing with leading edge protuberances to the situations with a wide range of attacking angle.



## REFERENCES

1. Fish F. E. & Battle J. M., *Hydrodynamic Design of the Humpback Whale Flipper*, *J. Morphology*, 1995, **225**, pp. 51-60.
2. Miklosovic, D. S. et al., *Leading-Edge Tubercles Delay Stall on Humpback Whale (Megaptera novaeangliae) Flippers*, *Physics of Fluids*, 2004, **16**, p. L39.
3. Bushnell, D. M. and Moore, K. J., *Drag Reduction in Nature*, *Annual Review of Fluid Mechanics*, 1991, **23**, pp. 65-79.
4. Watts, P. and Fish, F. E., *The Influence of Passive, Leading Edge Tubercles on Wing Performance*, *Proceeding of the Eleventh International Symposium on Unmanned Untethered Submersible Technology*, 2001.
5. Stein, B. and Murray, M. M., *Stall Mechanism Analysis of Humpback Whale Flipper Models*, *Proceeding of Unmanned Untethered Submersible Technology (UUST)*, UUST05, Durham, New Hampshire, August 2005.
6. Johari, H.; Henocho, C. H.; and Custodio, D., *Visualization of Flow on Hydrofoils With Leading Edge Protuberances*, ISFV13, 2008.
7. Van Nierop, E.; Alben, S.; and Brenner, M., *How Bumps on Whale Flippers Delay Stall: An Aerodynamic Model*, *Physical Review Letters*, 2008, **100**, 054502.
8. Pedro, H. T. C., *Determination of the Aerodynamic Characteristics of Low Reynolds Number Flows over Small Uninhabited Aerial Vehicle*, University of Hawaii, 2008.
9. Levshin, A.; Custodio, D.; Henocho, C.; and Johari, H., *Effects of leading edge protuberances on airfoil performance*, *AIAA Journal*, 2007, **45(11)**, pp. 2634–2642.
10. Pedro, H T.C. and Kobayashi, H. M., *Numerical Study of stall delay on humpback whale flippers*, paper 2008-0584, 46th AIAA Aerospace Sciences Meeting and Exhibit, 7–10 January, 2008.
11. Weber, P. W.; Howle, L. E.; and Murray, M. M., *Lift, Drag, and cavitation onset on rudders with leading-edge tubercles*, *Marine Technology*, 2010, **47(1)**, pp. 27–36.
12. Miklosovic, D. S.; Murray, M. M.; Howle, L. E., *Experimental evaluation of sinusoidal leading edges*, *Journal of Aircraft*, 2007, **44(4)**, pp.1404–1407.